Electric Power Systems Research 225 (2023) 109871

Contents lists available at ScienceDirect

Electric Power Systems Research

journal homepage: www.elsevier.com/locate/epsr

Fault location algorithm for distribution systems with distributed generation based on impedance and metaheuristic methods

André Luís da Silva Pessoa *, Mário Oleskovicz

University of São Paulo, São Paulo, Brazil

ARTICLE INFO

Keywords:
Distribution system
Distributed generation
Fault location
Impedance-based method
Metaheuristic

ABSTRACT

The growing penetration of distributed generators results in a bidirectional power flow in electrical power systems, especially in distribution systems. In this context, technologies and applications already developed and consolidated aimed at the operation and protection of methods should be reassessed. In this context, this research proposes developing a fault location algorithm for distribution systems with distributed generation. The main objective is to estimate the fault distance and fault resistance. The implemented algorithm consists of using meters present in the distribution system, such as, for example, in the substation and next to the distributed generators, to calculate from the system impedance information, and using a meta-heuristic algorithm, the resistance and the distance of the short-circuit. The methodology developed brings a differential in estimating the distance and resistance of the fault in parallel using meta-heuristic algorithms, using a relatively simple methodology that does not require the calculation of load flows in the system. Several sensitivity tests were considered in evaluating the proposed methodology, such as changes in the type, application position, fault resistance, post-fault data window considered, variation in the quantity and placement of allocated distributed generators, and the impact of the lack of synchronism between the data used. The results obtained are promising for estimating fault distance and fault resistance.

1. Introduction

Faults, or short circuits, in distribution systems, are considered the leading causes of interruption in electricity supply to system users and are responsible for disturbances in power quality [1]. One of the ways that can be effective in improving these indices is by developing and applying algorithms for the location of short circuits. Since the more quickly and accurately they are located, the electrical system can be promptly reestablished, reducing the time of discontinuity of supply and resulting damages.

In general, fault location algorithms for distribution systems are based on fault impedance. In general, these methods are categorized as methods based on lumped network parameters (*lumped-parameters*), techniques with the representation of network sections by quadrupoles, and methods based on data from fault recorders (*fault-recorders*). In addition to the classical methods, there are alternative ways to solve the problem that involve the use of intelligent systems (such as, for example, artificial neural networks, fuzzy systems, and expert systems) and meta-heuristics, such as genetic algorithms [2].

In addition to these considerations, the fault resistance calculation, resulting from the proposed methodology, can also be better explored in future works for other functions applied to distribution systems. The fault resistance is an essential element for short-circuit analysis methods used by protection engineers since it allows the estimation of the short-circuit current and voltage levels and thus allows a proper parameterization of the fault resistance algorithms, ensuring, for example, coordination of protection [3].

As for research on fault location in distribution systems, it is worth highlighting some of the works mentioned. Of these, it is essential to emphasize that many of the factors pointed out in [4] were not contemplated in a simplified way. For example, in [5], it is found an approach based on impedance but focusing only on one type of fault in a system with low complexity and penetration of DG (Distributed Generation). In [6], there is an approach based on machine learning to identify both the fault distance and the faulted system region. [7] considered an approach based on system sequence components to estimate the fault distance. [8] use an impedance-based approach, using information from both the substation and the DG installation locations. [1] presents an impedance-based method that considers the data from the substation and the buses containing DG synchronized via GPS. In addition, an algorithm is used to estimate the state of all system loads. [9] heuristic methods were used to locate the fault. [10] denote

* Corresponding author.
E-mail addresses: alsp@usp.br (A. da Silva Pessoa), olesk@sc.usp.br (M. Oleskovicz).

https://doi.org/10.1016/j.epsr.2023.109871
Received 12 July 2023; Received in revised form 1 September 2023; Accepted 19 September 2023
Available online 5 October 2023

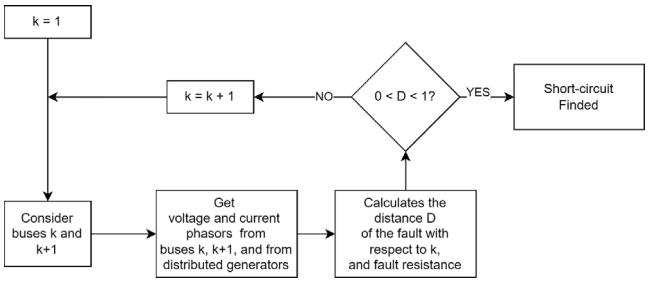

Fig. 1. Methodology flowchart for short-circuit location and fault resistance estimation.

the heavy use of PMUs (Phasor Measurement Units) installed in the system and divide the localization strategy into detecting the faulted section and estimating the fault distance. In [11], the faulted system region is detected based on information from the circuit breakers. [12] use support vector machines to identify the faulty areas, and [13] infer about the faulty section through the positive and negative sequence components. [14] presents the use of waveforms and signal energies to detect missing sections. [15] uses genetic algorithms to allocate intelligent electronic devices to support fault location efficiently. [16] brings light to two approaches to fault location that use artificial neural networks and traveling waves, in which the financial aspects for implementing each strategy are presented, among other things. In [17], an Adaptive Neuro-Fuzzy Inference System was used in a 20 kV distribution system. Finally, [18] also detect the missing regions using *deep learning* models.

This article proposes estimating fault distance and resistance using an impedance-based algorithm with the support of metaheuristic algorithms. The implemented algorithm consists of using meters present in the system, such as, for example, in the substation and next to the distributed generators, calculating from the information of the system impedance, and using a meta-heuristic algorithm, the resistance and the distance of the short circuit. Several sensitivity tests are presented that reflect, among other things, the impact of distributed generation on the methodology. The simulations considered the 34-buses IEEE distribution system [19] and the CIGRÉ system [20]. In each, distributed generators were allocated, and several tests were performed to understand how the proposed algorithm behaves in the face of these sensitivity tests. The literature lacks studies on the impact of the number and positioning of distributed generators and the lack of synchronism between the electricity meters used to locate short circuits. This article also presents tests taking these scenarios into account. Based on the results obtained, the proposed methodology allows good obtaining of distance and short-circuit resistance information.

2. Methodology

This section will present the methodology for estimating the distance and the short circuit's resistance. Fig. 1 summarizes the steps followed. Throughout this section, the details behind this process will be detailed.

For this item, the modeling of a distribution line found in [21] will be presented again. Next, the considerations about the proposed algorithm for estimating resistance and fault location will be shown.

Estimating the fault resistance will be essential for this application because the short-circuit modeling in the system considers both the location of the fault occurrence and the fault resistance. Thus, in the localization process, both information is obtained through the developed methodology.

Fig. 2 presents the electrical model referring to a section of a line of any distribution system.

Applying Kirchhoff's current law at node m:

$$\left[I_{line}\right]_{abc} = \left[I_{abc}\right]_m + 1/2[Y_{abc\,n-m}]\left[V_{LG}\right]_{abc}. \tag{1}$$

In which:

$$\left[I_{line}\right]_{abc} = \begin{bmatrix} I_{line\,a} \\ I_{line\,b} \\ I_{line\,c} \end{bmatrix}_n, \tag{2}$$

$$\left[I_{abc}\right]_m = \begin{bmatrix} I_{a\,m} \\ I_{b\,m} \\ I_{c\,m} \end{bmatrix}_m, \tag{3}$$

$$\left[V_{LG\,abc}\right]_m = \begin{bmatrix} V_{ag} \\ V_{bg} \\ V_{cg} \end{bmatrix}_m, \text{ and} \tag{4}$$

$$\left[Y_{abc}\right]_{abc} = \begin{bmatrix} Y_{aa} & Y_{ab} & Y_{ac} \\ Y_{ba} & Y_{bb} & Y_{bc} \\ Y_{ca} & Y_{cb} & Y_{cc} \end{bmatrix}. \tag{5}$$

where

$$[a] = [U] + 1/2[Z_{abc\,n-m}][Y_{abc\,n-m}] \tag{6}$$

$$[b] = [Z_{abc\,n-m}], \tag{7}$$

$$[c] = [Y_{abc\,n-m}] + 1/4[Y_{abc\,n-m}][Z_{abc\,n-m}][Y_{abc\,n-m}], \tag{8}$$

$$[d] = [U] + 1/2[Z_{abc\,n-m}][Y_{abc\,n-m}], \tag{9}$$

and

$$\begin{cases} \left[V_{LG\,abc}\right]_m = [a]\left[V_{LG\,abc}\right]_n - [b]\left[I_{abc}\right]_n \\ \left[I_{abc}\right]_m = -[c]\left[V_{LG\,abc}\right]_n + [d]\left[I_{abc}\right]_n \end{cases}. \tag{10}$$

Initially, the algorithm will be applied to the first stretch of line in the system between the reference slash k and the slash $k + 1$. Thus, for $k = 1$, it will be between Bars 1 and 2. Thus, $Z_{abc\,01-02}$, $Y_{abc\,01-02}$, and $Z_{abc\,01-02}$, and Z_{BUS}. A cycle of voltage and postfault current signals from the reference bus and the bus, or buses, will be considered on which distributed generation is installed.

To obtain the voltage and current phasors for the three-phase signals of Bus 1, post-fault cycle windows will be used in conjunction with the Discrete Fourier Transform (DFT). This method can also be applied to the buses containing distributed generation, as shown in Fig. 3.

The fault location algorithms based on impedance present a strategy for searching the system, and the algorithm that will be presented and implemented also follows this line. Initially, the first section of the system from the substation is analyzed. It is evaluated whether the fault occurred in this section or another section of the system. Thus, this algorithm has two steps. The first is to apply it to the first section and the second to other system sections. This algorithm considers as available information, in addition to the impedance and admittance matrices *shunt* of the system, the three-phase voltage and current signals referring to Bus 01, as well as the three-phase current signals coming from the distributed generators installed in the system. In this way, the mathematical development to estimate the position of the faults in the possible sections of the system will take these assumptions into account.

Based on Fig. 3:

$$\begin{matrix} \left[V_{LG\,abc}\right]''_{02} = [a]\left[V_{LG\,abc}\right]'_{01} - [b]\left[I_{abc}\right]'_{01} \\ \left[I_{abc}\right]''_{02} = -[c]\left[V_{LG\,abc}\right]'_{01} + [d]\left[I_{abc}\right]'_{01} \end{matrix}. \tag{11}$$

In which:

$$[a] = [U] + 1/2[Z_{abc\,01-02}][Y_{abc\,01-02}], \tag{12}$$

$$[b] = [Z_{abc\,01-02}], \tag{13}$$

$$[c] = [Y_{abc\,01-02}] + 1/4[Y_{abc\,01-02}][Z_{abc\,01-02}][Y_{abc\,01-02}], \tag{14}$$

and

$$[d] = [U] + 1/2[Z_{abc\,01-02}][Y_{abc\,01-02}]. \tag{15}$$

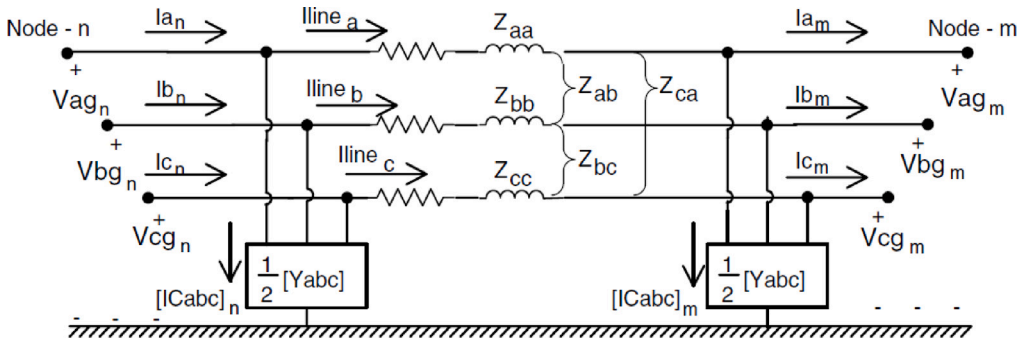

Fig. 2. Electrical model of distribution system section [21].

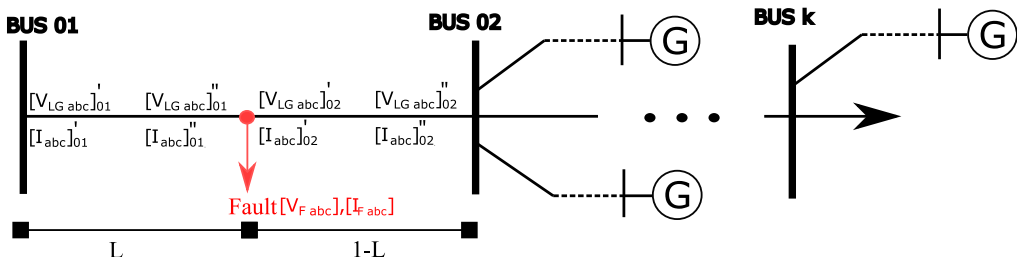

Fig. 3. Electrical model of a distribution system considering the presence of distributed generation and a short circuit.

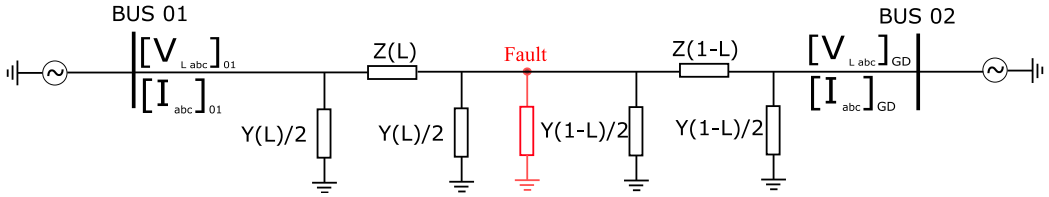

Fig. 4. Simplified representation of the faulted section, considering the presence of distributed generation and fault resistance.

Considering a solid fault applied at a distance D from $Bar\,01$, the voltage $[V_{F\,abc}]$ will be:

$$\left[V_{F\,abc}\right] = [a(D)]\left[V_{LG\,abc}\right]'_{01} - [b(D)]\left[I_{abc}\right]'_{01}, \tag{16}$$

for

$$[a(D)] = [U] + 1/2L^2[Z_{abc\,01-02}][Y_{abc\,01-02}] \tag{17}$$

and

$$[b(D)] = [Z_{abc\,01-02}(D)] = D[Z_{abc\,01-02}]. \tag{18}$$

However, Eq. (16) does not represent well the effect of fault resistance in the calculation of $\left[V_{F\,abc}\right]$, and not even the impact of distributed generation. For each type of fault (Phase-to-Ground - PG, Phase-to-Phase - PP, Phase-to-Phase-to-Ground - PPG, Three-Phase - PPP, and Three-Phase-to-Ground - PPPG), the fault resistance $[R]$ is represented according to Table 1. Table 1 is used through a previous fault type classification step. It should be noted that fault-type classification was not the focus of this approach; therefore, this methodology assumes that this classification has already been carried out.

Considering distributed generation as a current source and also the effect of fault resistance, Fig. 3 will be redone (and giving rise to Fig. 4) assuming the fault occurring between the Buses 01 and 02.

From the simulations carried out using the PSCAD software, considering the analysis of several applied short-circuit situations, we arrived

Table 1
Representation of $[R]$ according to the phases directly involved in the fault.

Fault type	Representation for $[R]$
AG	$\begin{bmatrix} R & 0 & 0 \\ 0 & 0 & 0 \\ 0 & 0 & 0 \end{bmatrix}$
BG	$\begin{bmatrix} 0 & 0 & 0 \\ 0 & R & 0 \\ 0 & 0 & 0 \end{bmatrix}$
CG	$\begin{bmatrix} 0 & 0 & 0 \\ 0 & 0 & 0 \\ 0 & 0 & R \end{bmatrix}$
AB or ABG	$\begin{bmatrix} R & R & 0 \\ R & R & 0 \\ 0 & 0 & 0 \end{bmatrix}$
BC or BCG	$\begin{bmatrix} 0 & 0 & 0 \\ 0 & R & R \\ 0 & R & R \end{bmatrix}$
AC or ACG	$\begin{bmatrix} R & 0 & R \\ 0 & 0 & 0 \\ R & 0 & R \end{bmatrix}$
ABC or ABCG	$\begin{bmatrix} R & R & R \\ R & R & R \\ R & R & R \end{bmatrix}$

at (16) in Eq. (19), in which it was possible to emulate the effect of distance and resistance of the fault on $\left[V_{F\,abc}\right]$:

$$\left[V_{F\,abc}\right] = [a(D)]\left[V_{LG\,abc}\right]'_{01} - ([b(D)] + [R])\left[I_{abc}\right]'_{01} - [R]\sum_{i=1}^{N}[I_{abc\ GD}]_i, \ . \tag{19}$$

where $\sum_{i=1}^{N}[I_{abc\ GD}]_i$ is the sum of all N phasors of the generators downstream of the section under analysis.

During the occurrence of the fault, depending on the value of the fault resistance, a greater or lesser part of the upstream current, as well as the downstream current, will pass through the short circuit. In this way, being $pinv(*)$ the pseudo-inverse operator, α and β are defined as:

$$\alpha = (Z(1-D) + [Z]_D) * pinv(Z(1-D) + [R] + [Z]_D), \ and \tag{20}$$

$$\beta = (Z(D) + [Z]_U) * pinv(Z(D) + [R] + [Z]_U). \tag{21}$$

$[Z]_D$ represents the equivalent impedance upstream of the section under analysis, and $[Z]_U$ is the equivalent impedance downstream of the section. $[Z]_D$ is calculated by multiplying the distance between the substation and the hypothetical fault location by the average impedance of all three-phase sections of the system, and $[Z]_U$ is calculated by multiplying the distance between the hypothetical fault location and the remainder of the most significant three-phase section downstream of the fault by the average impedance of all three-phase sections in the system.

Thus, α and β will weigh the contribution of the substation and the DG in the fault according to the short-circuit resistance. For a short-circuit resistance tending to zero, α and β will tend to 1 (100% of the currents coming from the substation and the DGs will be considered). For a short-circuit resistance tending to infinity α and $beta$ will tend to 0 (0% of the currents coming from the substation and the DGs will be considered). In this way, the voltage at the hypothetical fault point will be deemed to be:

$$\left[V_{F\,abc}\right] = [a(L)]\left[V_{LG\,abc}\right]'_{01} - ([b(L)] + [R])\alpha\left[I_{abc}\right]'_{01} - [R]\beta\sum_{i=1}^{N}[I_{abc\ GD}]_i \ . \tag{22}$$

It is worth clarifying that in Eq. (22), the objective was to make the proposed mathematical model more sensitive to the fault resistance value. Thus, the addition of alpha and beta terms was made. The idea behind alpha and beta was to bring the concept of a current divider into Eq. (19) so that for a huge fault resistance, a tiny fraction of the current from the substation (or distributed generators) will contribute to the short circuit.

In this way, the calculation of $\left[V_{F\,abc}\right]$ depends on D and R, which are initially unknown variables.

In this work, it is proposed to determine the location of occurrence of the fault by observing the behavior of $\left[V_{F\,abc}\right]$ with the variation of D and R.

Thus, the algorithm will start its estimation from the first section of the substation, setting D and R equal to zero. For each value of D and R, $\left[V_{F\,abc}\right]$ is calculated. After that, R is kept, and D is incremented by a given value, obtaining:

$$D = D + \Delta D. \tag{23}$$

This process will repeat until

$$D \leq D_{sup}. \tag{24}$$

After D reaches this upper limit, the process is redone to

$$R = R + \Delta R \tag{25}$$

until

$$R \leq R_{sup}. \tag{26}$$

At each simulation, the value of $max(abs(\left[V_{F\,abc}\right]))$ of the phases directly involved in the fault will be saved. The fault will then be located for the situation of (R, D) that presents the smallest value of $max(\left[V_{F\,abc}\right])$. To optimize the search for D and R values, metaheuristic algorithms were used to obtain these values.

As for the choice of the metaheuristic to be used, tests were carried out using the Genetic Algorithm [22], Particle Swarm Optimization (*Particle Swarm Optimization*) [23], and Simulated Annealing (*Simulated Annealing* - SA) [24]. These algorithms were used from [25]. The metaheuristic is used to minimize the objective function defined as max(abs([VF abc])). Thus, it offers adequate support in choosing the value of D and R that minimizes this expression. In this sense, three different meta-heuristics were tested in this article to observe the impact of using different algorithms in obtaining D and R. The meta-heuristics were chosen based on the implicit characteristics of each methodology, adapting them to the desired objective function. In the fault location process, both the fault distance (D) and the fault resistance are calculated sequentially by the metaheuristic optimization algorithm.

The SA algorithm was chosen for the general tests because it has an excellent problem-solving capacity and can avoid local minima. However, as will be demonstrated in the experiments, other meta-heuristics can be used so that the fault locator still maintains a suitable identification of D and R.

3. Results

In this section, the results obtained will be presented. The results refer to two distribution systems with different characteristics. The presented results consider the average error and the standard deviation of all the stretches in the respective test systems used to validate the exposed methodology.

3.1. Results for the 34-bus IEEE distribution system

To exemplify and denote the potentiality of the proposed methodology, in the experiments reported in detail, the 34-bus IEEE distribution system [19] will be used, represented in Fig. 5 with its original notation for each one of the bars. For modeling the distribution system (using the *software PSCAD™/EMTDC™* [26]), the voltage regulators were removed. It is worth mentioning that, although they were disregarded in the simulations, both the voltage regulators and the loads and lateral branches were considered in the definition of the system sections. Two wind turbines with fixed speed (positioned according to the IEEE system naming standard of 34 buses on buses 852 and 848) were also added, with electrical characteristics and placements as found in [27]. The wind turbine is Type III, with converters in the medium [26] model. All loads were modeled as constant impedance.

In the simulations carried out in this system, short circuits were applied in the three-phase sections every 1 km and also considered short circuits with fault resistance of 0 Ω, 25 Ω, 50 Ω, 100 Ω, 200 Ω, 500 Ω, and 1000 Ω. In addition, all 11 types of faults (single-phase, two-phase, two-phase-ground, three-phase, and three-phase-ground) were considered. It was considered 256 samples per cycle. The white noise of 48 dB was added to all simulated three-phase voltage and current signals to better characterize the three-phase voltage and current signals. This value of 48 dB was chosen since, according to [28,29], the noise in measuring equipment is typically between 70 dB and 48 dB. In all, 420 simulations were applied to the system for each type of fault.

The following lower and upper bounds were adopted for R and D:

$$0\ \Omega\ < R < \ 1.000\ \Omega;\ and \tag{27}$$

$$0\ <\ D\ <\ 1. \tag{28}$$

Such variables represent the resistance of the fault (R) and the distance of the fault at the beginning of a section of the system (D).

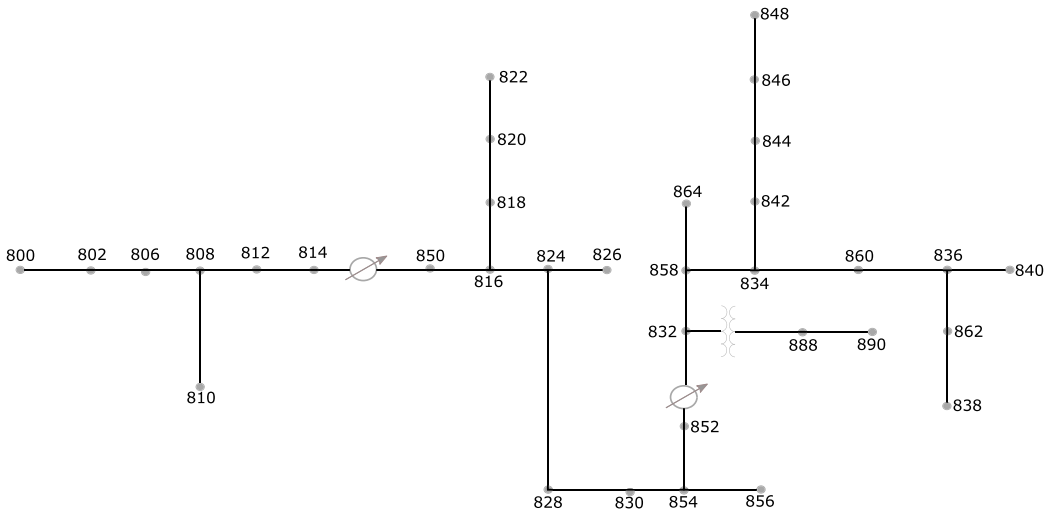

Fig. 5. 34-buses distribution system.

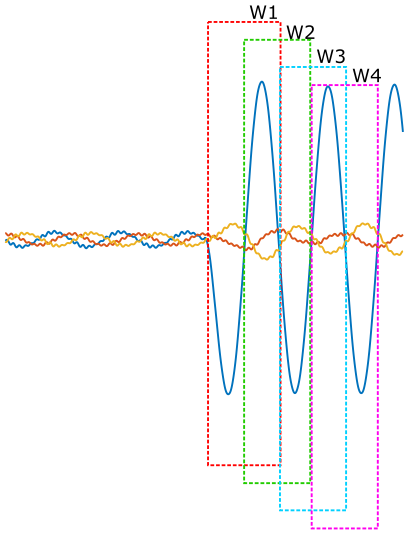

Fig. 6. Parsed post-fault data windows.

Table 2
Performance of the proposed algorithm when varying the post-fault data window.

Fault type	Mean error (km)	Standard deviation
W1	2.54	1.68
W2	0.21	0.36
W3	0.28	0.27
W4	**0.21**	**0.16**

Table 3
General performance of the proposed algorithm when varying the fault type.

Fault type	Mean error (km)	Standard deviation
AG	0.21	0.16
BG	1.00	0.62
CG	1.40	0.58
AB	1.96	1.24
BC	0.70	0.67
AC	0.43	0.38
ABG	0.96	1.00
BCG	0.25	0.16
ACG	0.24	0.17
ABC	0.54	0.36
ABCG	0.51	0.38

Thus, for each simulated short circuit, the section where the fault distance D is between 0 and 1 is searched when scanning the system sections. The search universe for fault resistance is between 0 and 1000 Ω to observe in the results how the algorithm behaves for very high values of fault resistance.

3.1.1. The effect of the chosen post-fault data window and fault type

This section considers several post-fault data windows to evaluate the algorithm's performance. Several tests are performed to observe the effect of the post-fault data window and the *DC* component of exponential decay on the algorithm's performance. A single-phase short circuit (phase A to ground) with fault resistance of 25 Ω was considered.

Fig. 6 presents all post-fault data windows used, where *W1* represents the first post-fault data window, considering a cycle based on the fundamental frequency (60 Hz), being the other windows (W2, W3, and W4) obtained from a half-cycle displacement of this first one. A sampling rate of 256 samples/cycle was considered.

Table 2 presents the algorithm's performance for each considered window. Are presented for each window about the error (in km), the mean, and the standard deviation, respectively. It is observed that the windows that offered the best performance for the algorithm were *W4* and *W2*, with *W4* being the best of all those evaluated (based on the mean and deviation default calculated). A justification for this behavior stems from the probable decrease in the oscillatory transient caused by the fault situation already in this *W4* window.

3.1.2. Fault type effect

Next, it shows how an unbalanced distribution system can interfere with the algorithm's performance against different types of faults. The presented results consider R_g equal to 25 Ω and the window *W4*, with a sampling frequency of 60 Hz (256 samples per cycle).

Table 3 summarizes the locator's statistical data for each of the 11 applied fault types. The algorithm's performance changes according to the kind of fault, which is consistent with the strongly unbalanced tested system.

3.1.3. Effect of fault resistance

Fig. 7 shows the algorithm's performance for different values of R_g ranging from 0 Ω to 1000 Ω. For faults of up to 100 Ω, there is a satisfactory correlation between the estimated fault distance and the actual fault distance. For faults with R_g of 200, 500, and 1000 Ω, there is a total saturation in the estimated distance of the fault. Thus, the proposed algorithm satisfactorily meets up to 100 Ω shortages. It is worth noting that good performance is presented by the algorithm up

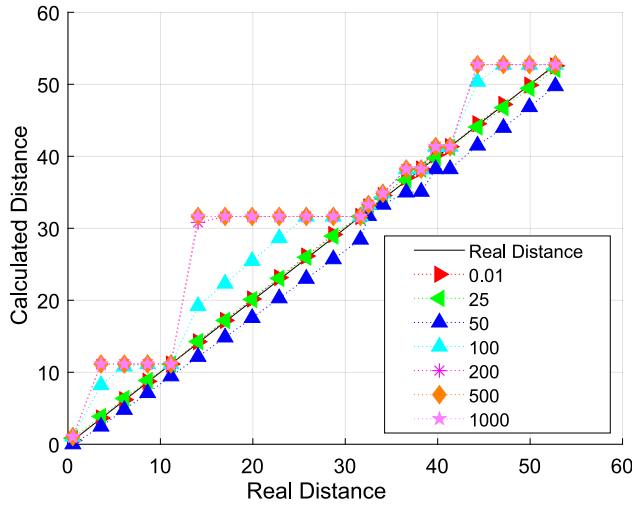

Fig. 7. Performance of the algorithm in estimating the distance of a single-phase A to ground short circuits for R_g of 0, 25, 50, 100, 200, 500, and 1000 Ω.

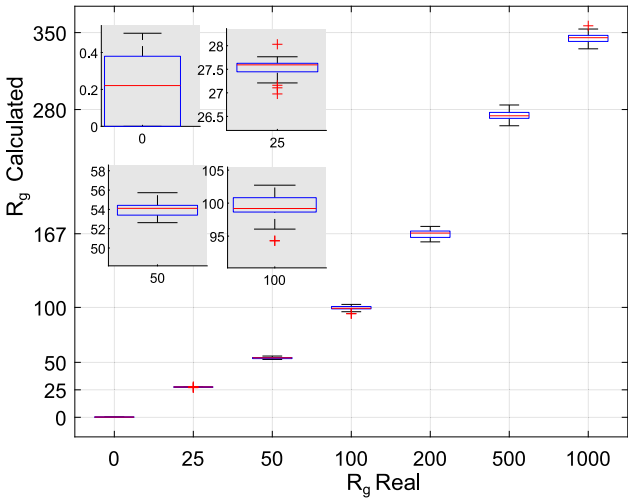

Fig. 9. Algorithm performance in estimating the resistance of a single-phase A to ground short circuits for R_g from 0, 25, 50, 100, 200, 500, and 1000 Ω.

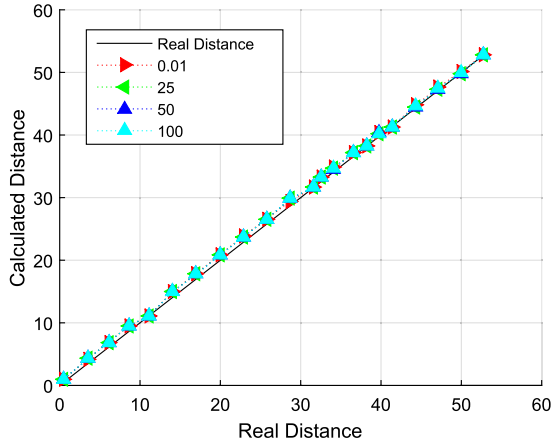

Fig. 8. Performance of the algorithm in estimating the distance of a three-phase-to-earth short circuits for R_g of 0, 25, 50, and 100 Ω.

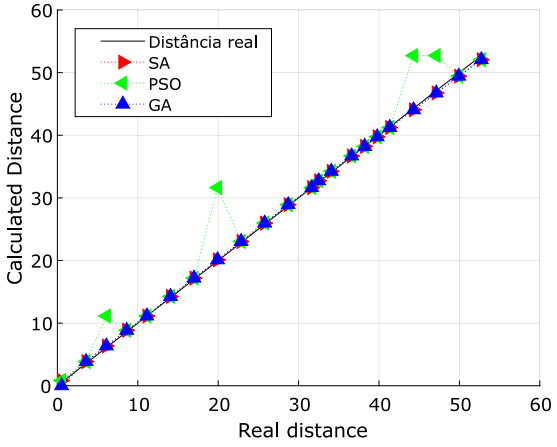

Fig. 10. Algorithm performance in estimating the distance of a single-phase A to ground short circuit with R_g of 25 Ω when using different meta-heuristics.

to a fault resistance of 50 Ω [30]. Fig. 8 shows the behavior of the fault locator for three-phase-to-earth faults considering different values of fault resistance. It is observed that, regardless of the fault resistance adopted in the simulations, the algorithm's behavior remains the same for this fault type.

It is worth noting that the algorithm also estimates the fault resistance in addition to the fault distance. Fig. 9 shows the estimation of the fault resistance of the implemented algorithm for several tested values (in detail, observe the zoom given to the *boxplots* of the estimates of faults with a value of R_g from 0, 25, 50 and 100 Ω). It is observed that the algorithm estimates well up to R_g of 100 Ω. An exemplary fault resistance identification was not observed for the tests with R_g of 200, 500, and 1000 Ω. Thus, the values returned for 200, 500, and 1000 Ω fault resistors were 167, 280, and 350 Ω.

The chosen meta-heuristic for the identification of D and R

Fig. 10 shows the performance in estimating fault distance for the different metaheuristics used. It is observed that, in general, the SA, AG, and PSO have the same performance. However, the PSO presented some cases with high errors. It is worth mentioning that for these tests, the algorithms available in Matlab [25] were used in their standard form without any improvements.

Table 4
Algorithm performance in estimating the distance of a single-phase A to ground short circuits with R_g of 25 Ω when considering two DGs with different placements.

	Average error (km)	Standard deviation
852, 848	0.2104	0.1573
832, 834	0.1847	0.1494
MID-834, 836	0.1306	0.1120

3.1.4. *Effect of increasing the number and positioning of DGs*

For this experiment, four scenarios were considered for positioning the DGs. These scenarios are organized into two groups. The first group focused on the presence of two DGs and performed a variation in their positioning. In the second group of experiments, three DGs and variations in their positions are also performed. It is also worth noting that the total active power injection of the DGs was respected in all tests according to [27].

In the tests focused only on the variation in the positioning of the DGs, modifications were made in the position of the two wind turbines in the first group so as not to disrespect the original allocation too much. The following positions were considered: at bars 832 and 834 and MID-834 and 836. Table 4 presents the results obtained for each considered case.

Table 5
Performance of the algorithm in estimating the distance of a single-phase A to ground short circuits with R_g of 25 Ω when considering three GDs.

	Average error (km)	Standard deviation
852, 848	0.2104	0.1573
852, 832, 834	0.1877	0.1316
852, MID-834, 836	0.1855	0.1298

Table 6
Performance of the algorithm in estimating the distance of a single-phase A to ground short circuits with R_g of 0 and 25 Ω, when considering and disregarding the synchronism between the measured signals.

	R_g = 0 Ω		R_g = 25 Ω	
	Mean	Standard deviation	Mean	Standard deviation
With sync	0.18	0.17	0.21	0.16
No sync	0.21	0.29	6.64	5.64

Table 7
Performance of the proposed algorithm when varying the fault type in the test system under analysis.

	Mean error (km)	Standard deviation
AG	0.20	0.32
BG	0.20	0.33
CG	0.20	0.33
AB	0.56	0.33
BC	0.30	0.16
AC	0.31	0.16
ABG	0.24	0.12
BCG	0.24	0.20
ACG	0.25	0.20
ABC	0.25	0.17
ABCG	0.25	0.17

Three DGs were considered in the system in the second group of tests. One was considered in position 852 (according to the original allocation), and the other followed the positions made in the experiments with two previously mentioned DGs. In one of these scenarios, the DGs are positioned at nodes 852, 832, and 834; in another scenario, the DGs are allocated at nodes 852, MID-834 (positioned between bars 858 and 834), and 836. In Table 5 are results for estimating the missing distance of these scenarios compared to the standard allocation (852 and 848).

According to the presented results, there is a sensitivity of the fault locator in the position variation and the number of DGs being observed, even reducing the average error of the estimated fault distance. A minor reduction of errors was also observed compared to DGs positioned in **852**, **MID-834**, **836**. It is then evident that the position of the distributed generators affects the result of the fault locator, and the quantity is also a factor that can impact the algorithm's results. It is also evident that in the scenario with three DGs, even with changes in the positions of the generators, it is possible to have similar results.

3.1.5. Experiments involving loss of synchronism between signals coming from distributed generators

In this experiment, the signals from the generator positioned at bus 852 and 848 ahead (out of phase) by a quarter of a cycle about the substation were considered. Table 6 presents the results obtained for the scenarios with and without synchronism. It is evident that for the situation without fault resistance, the results are still similar, but when considering a fault resistance of 25 Ω, the lack of synchronism significantly compromises the fault locator.

3.2. Results for the CIGRÉ distribution system

As part of the tests carried out considering the proposed methodology, the microgrid formed from the CIGRÉ test system (Conseil International des Grands Réseaux Electriques) [20], represented in

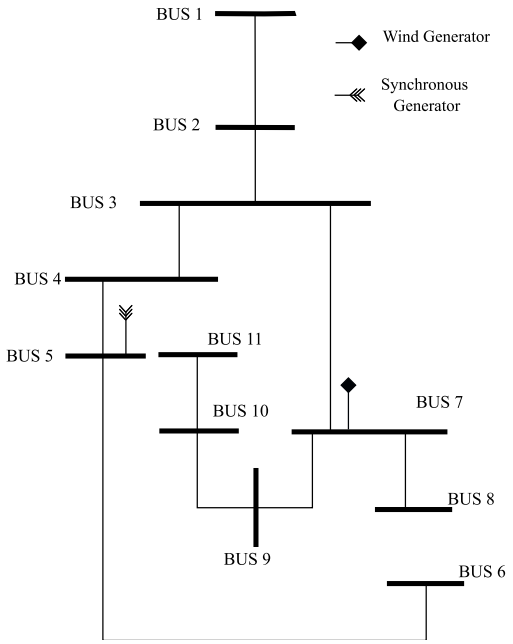

Fig. 11. Microgrid modeled from CIGRÉ test system.

Fig. 11, was used. In this system, two generators were allocated. They are characterized by a synchronous generator (injecting 5 MW of active power into the system) and a fixed-speed wind turbine (injecting 2 MW of active power into the system). For this system, faults were applied at most every 400 m from the feeders. The resistance between phases and ground from 0 Ω to 50 Ω was considered, and all 11 types of short circuits were applied. Three hundred twenty simulations were used in the system for every fault.

Table 7 summarizes the performance of the fault location algorithm for each of the 11 fault types when considering a short-circuit resistance of 0 Ω. Paralleling with the 34-bus IEEE distribution system, there is more excellent stability here for faults of the same type. For example, phase A-ground, B-ground, and C-ground faults have similar results. It is observed because the CIGRÉ system is much more balanced.

Fig. 12 presents the estimation of the fault resistance calculated by the algorithm for several tested values (observe in detail by *zoom* the *boxplots* of the fault estimates with a value of R_g from 0 Ω, 5 Ω, 10 Ω, 15 Ω, 20 Ω, 25 Ω, and 50 Ω). It is observed that the algorithm has a good estimation, at least up to the fault resistance of 25 Ω. A suitable fault resistance identification was not observed for tests with fault resistance of 50 Ω. A value around 29.21 Ω was returned for this resistance.

4. Conclusions

This article presents a method for locating faults in distribution systems using an approach that makes use of system impedance information and meta-heuristic techniques. Various sensitivity tests were performed.

It was found that the post-fault window used favors the algorithm, which in this case was the window farthest from the instant of occurrence of the fault (which in this case was the fourth). It is possible to obtain a strong correlation of the estimated distance with the actual fault distance for a range of resistance values.

As for the estimation of the fault resistance, it was noted that the developed algorithm makes a good follow-up for resistance values more significant than those observed in the fault distance estimation. Thus, while the measure of the fault distance saturates for a given

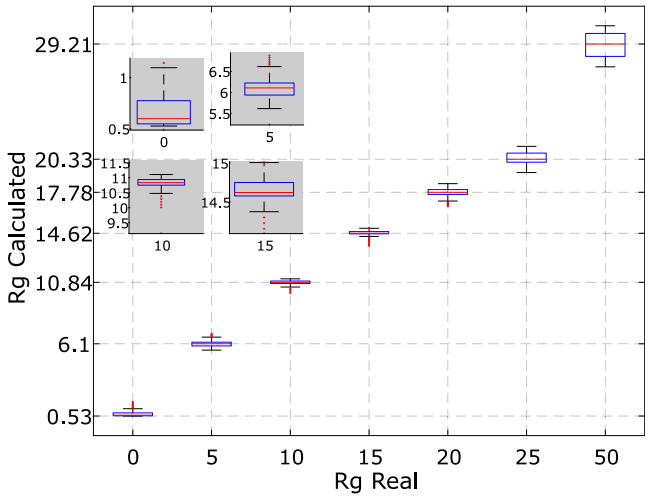

Fig. 12. Performance of the algorithm in estimating the resistance of a single-phase A to ground faults for R_g from 0 Ω, 5 Ω, 10 Ω, 15 Ω, 20 Ω, 25 Ω, and 50 Ω.

fault resistance, the assessment of this resistance saturates for faults with higher resistances. On faults without ground involvement, the algorithm will estimate a high fault resistance (around 200 Ω).

Experiments were performed with different metaheuristics, but the results were quite similar.

The number and placement of distributed generators may or may not significantly affect the algorithm's performance. Even with three generators distributed in the system, it is possible to have similar results with two meters allocated. The need for synchronism between the meters is critical for the proposed methodology. Even a slight loss of sync will have a significant impact on the results.

Declaration of competing interest

The authors declare the following financial interests/personal relationships which may be considered as potential competing interests: Andre Luis da Silva Pessoa reports financial support was provided by National Council for Scientific and Technological Development.

Data availability

The authors do not have permission to share data.

References

[1] S.F. Alwash, V.K. Ramachandaramurthy, N. Mithulananthan, Fault-location scheme for power distribution system with distributed generation, IEEE Trans. Power Deliv. 30 (3) (2015) 1187–1195.
[2] M.M. Saha, J.J. Izykowski, E. Rosolowski, Fault Location on Power Networks, Springer Science & Business Media, 2009.
[3] A.D. Filomena, M. Resener, R.H. Salim, A.S. Bretas, Distribution systems fault analysis considering fault resistance estimation, Int. J. Electr. Power Energy Syst. 33 (7) (2011) 1326–1335.
[4] S. Das, S. Santoso, A. Maitra, Effects of distributed generators on impedance-based fault location algorithms, in: 2014 IEEE PES General Meeting– Conference & Exposition, IEEE, 2014, pp. 1–5.
[5] J.d. Nunes, A.S. Bretas, Impedance-based fault location formulation for unbalanced primary distribution systems with distributed generation, in: Power System Technology (POWERCON), 2010 International Conference on, IEEE, 2010, pp. 1–7.
[6] H. Zayandehroodi, A. Mohamed, H. Shareef, M. Mohammadjafari, Determining exact fault location in a distribution network in presence of DGs using RBF neural networks, in: Information Reuse and Integration (IRI), 2011 IEEE International Conference on, IEEE, 2011, pp. 434–438.
[7] A. Bedoya-Cadena, C. Orozco-Henao, J. Mora-Florez, Single phase to ground fault locator for distribution systems with distributed generation, in: Transmission and Distribution: Latin America Conference and Exposition (T&D-la), 2012 Sixth IEEE/PES, IEEE, 2012, pp. 1–7.
[8] C. Orozco-Henao, J. Mora-Florez, S. Perez-Londono, A robust method for single phase fault location considering distributed generation and current compensation, in: Transmission and Distribution: Latin America Conference and Exposition (T&D-la), 2012 Sixth IEEE/PES, IEEE, 2012, pp. 1–7.
[9] G. Manassero, S.G. Di Santo, L. Souto, Heuristic method for fault location in distribution feeders with the presence of distributed generation, IEEE Trans. Smart Grid 8 (6) (2017) 2849–2858.
[10] T. Niu, X. Cheng, Y. Zhang, Z. Lu, Fault location method of distribution network based on multi-source information, in: 2020 IEEE International Symposium on Product Compliance Engineering-Asia (ISPCE-CN), IEEE, 2020, pp. 1–6.
[11] Q. Zhou, B. Zheng, C. Wang, J. Zhao, Y. Wang, Fault location for distribution networks with distributed generation sources using a hybrid DE/PSO algorithm, in: 2013 IEEE Power & Energy Society General Meeting, IEEE, 2013, pp. 1–5.
[12] R. Pérez, C. Vásquez, Fault Location in distribution systems with distributed generation using Support Vector Machines and smart meters, in: Ecuador Technical Chapters Meeting (ETCM), IEEE, Vol. 1, IEEE, 2016, pp. 1–6.
[13] Y. Li, G. Zou, J. Yang, H. Sui, Faulty section location scheme for distribution grid with inverter interfaced distributed generation, in: Innovative Smart Grid Technologies Conference Europe (ISGT-Europe), 2017 IEEE PES, IEEE, 2017, pp. 1–6.
[14] Y. Chang, J. Tang, Y. Li, B. Xiong, X. Lu, J. Liu, A novel single-phase-to-ground fault location method based on phase current differences in power distribution systems, in: 2022 4th International Conference on Smart Power & Internet Energy Systems (SPIES), IEEE, 2022, pp. 1196–1201.
[15] R. Muka, M. Garau, P.E. Heegaard, Genetic algorithm for placement of IEDs for fault location in smart distribution grids, 2021.
[16] H. Amiri, Analysis and comparison of artificial neural network and traveling wave algorithm for distribution networks fault location, in: 2023 5th International Conference on Optimizing Electrical Energy Consumption (OEEC), IEEE, 2023, pp. 1–5.
[17] M.B.R. Widodo, A. Soeprijanto, O. Penangsang, Analysis of fault location on distribution system using impulse injection learned by anfis, in: 2020 International Seminar on Intelligent Technology and Its Applications (ISITIA), IEEE, 2020, pp. 38–43.
[18] S. Liu, H. Yin, Y. Zhang, X. Liu, C. Li, Fault location method for distribution network with distributed generation based on deep learning, in: 2022 4th International Conference on Smart Power & Internet Energy Systems (SPIES), IEEE, 2022, pp. 1157–1162.
[19] D.T. Feeders, IEEE PES distribution system analysis subcommittee's, distribution test feeder working group, 2013.
[20] CIGRE, Technical brochure 575: Benchmark systems for network integration of renewable and distributed energy resources, 2014.
[21] W.H. Kersting, Distribution System Modeling and Analysis, CRC Press, 2012.
[22] D.E. Goldberg, P. Segrest, Finite Markov chain analysis of genetic algorithms, in: Proceedings of the Second International Conference on Genetic Algorithms, Vol. 1, 1987, p. 1.
[23] I.C. Trelea, The particle swarm optimization algorithm: convergence analysis and parameter selection, Inform. Process. Lett. 85 (6) (2003) 317–325.
[24] P.J. Van Laarhoven, E.H. Aarts, Simulated annealing, in: Simulated Annealing: Theory and Applications, Springer, 1987, pp. 7–15.
[25] M. MatLab, The Language of Technical Computing, The MathWorks, Inc., 2012, http://www.mathworks.com.
[26] M.H. Pscad, H. Pscad, Manitoba, research centre, 2005.
[27] R. Dugan, W. Kersting, Induction machine test case for the 34-bus test feeder-description, in: 2006 IEEE Power Engineering Society General Meeting, IEEE, 2006, p. 4.
[28] R.H. Tan, V.K. Ramachandaramurthy, Numerical model framework of power quality events, Eur. J. Sci. Res. 43 (1) (2010) 30–47.
[29] J.J. Tomic, M.D. Kusljevic, V.V. Vujicic, A new power system digital harmonic analyzer, IEEE Trans. Power Deliv. 22 (2) (2007) 772–780.
[30] M. Mirzaei, M. Ab Kadir, E. Moazami, H. Hizam, Review of fault location methods for distribution power system, Aust. J. Basic Appl. Sci. 3 (3) (2009) 2670–2676.